4M.5 IMPACT OF LAND SURFACE HETEROGENEITIES ON ATMOSPHERIC WATER VAPOR DISTRIBUTION DURING THE IHOP_2002 29 MAY 2002 CASE.

S. Bastin[1], P. Drobinski[2], C. Flamant[2], F. Chen[1], K. Manning[1]
1 National Center for Atmospheric Research, Boulder, CO, USA
2 Institut Pierre Simon Laplace/ Service d'Aéronomie, Paris, FRANCE

1. INTRODUCTION

The International H_2O Project (IHOP_2002) is a field experiment that took place in the South Great Plains of the United States of America during May-June 2002 (Weckwerth et al., 2004). It was dedicated to the study of the four-dimensional water vapor distribution in the atmosphere in order to improve the understanding and prediction of convection and associated rainfall.

The distribution of water vapor in the atmospheric boundary layer (ABL) is a determining factor in the processes of convection, producing or not precipitations. Thus, one necessary condition for an accurate prediction of convective rainfall is a good representation of the atmospheric water vapor in the models. However, mesoscale models still have some difficulties to represent correctly the water vapor distribution despite their capability to predict accurately most of the dynamical processes. The reason is that water vapor is undersampled in space and time (see for instance Weckwerth et al., 1996) although its variability is important due to a large variety of sources. In particular, the surface forcing, that is a source of water vapor via latent heat flux, has been underestimated in the models for a long time. The recent improvements in models, for instance the implementation of land surface models (LSM), are supposed to allow a better representation of the surface/atmosphere interactions.

This paper focuses on the 29 May 2002 case that was classified as a boundary layer heterogeneity (BLH) mission as part of the IHOP_2002 ABL component. The main focus of BLH missions was on determining the role soil moisture, natural or man-made land surface conditions and topography on the development of heterogeneities in the ABL moisture distribution. On 29 May 2002, strong heterogeneities of the boundary layer structure and water vapor mixing ratio in the ABL have been observed across the Oklahoma panhandle, in connection with inhomogeneities in soil moisture caused by heavy rains in the area during the night of 27 May 2002.

In this study, we use a combination of high-resolution observations (water vapor lidars, in particular) and numerical simulations (MM5 coupled with Noah land surface model initialized with the 40-km resolution NCEP Eta Data Assimilation System –EDAS- analyses for the atmosphere and with the products of a high-resolution land data assimilation system (HRLDAS; Chen et al., 2004) for the soil moisture and temperature) to identify the different sources of the water vapor variability in the atmosphere (namely surface forcing, including soil moisture and land use, and advection). To achieve this goal, the degree of correlation between the variables that characterize the surface state (for instance the latent heat flux, the soil moisture, the fraction of vegetation…) and the ABL water vapor and depth are analyzed.

2. OBSERVATIONS AND MODEL SET-UP

2.1 Observations

The IHOP_2002 field project took place over the Southern Great Plains of the continental U.S., with primary focus on the Texas Panhandles, Oklahoma and Kansas (see Figure 1).

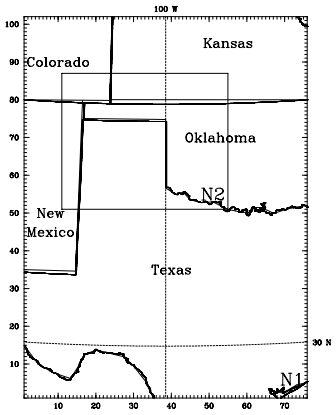

Figure 1: MM5 model domain for 12-km outer nest 1 (N1) and the location of 4-km inner nest 2 (N2).

IHOP_2002 took advantage of already existing networks and facilities in the area and IHOP_2002-specific fixed and mobile ground based sensors supplemented the operational measurements sites. In addition to the ground based sites, six research aircraft participated in IHOP_2002, all but one with remote sensing instrumentation (see Weckwerth et al., 2004 for more details). Extensive observational data for the entire IHOP_2002 period are available

through the field catalog located at http://www.joss.ucar.edu/catalog. The routine and special observational datasets used for the validation of this case study include University of Oklahoma mesonet data, the National Weather Service (NWS) soundings and surface observations, as well as two airborne water vapor differential absorption lidars (DIAL), the Deutsches Zentrum für Luft- und Raumfahrt (DLR) DIAL (Poberaj et al., 2002) and the Centre National pour la Recherche Scientifique (CNRS) DIAL LEANDRE2 (Bruneau et al., 2001). The locations of the numerous surface stations and the soundings platforms are indicated on Figure 2.

The CNRS DIAL was flown onboard of the Naval Research Laboratory (NRL) Orion P3 encompassed a region around Homestead (OK) doing several west to east legs in the Texas and Oklahoma panhandle between 1630 and 2112 UTC. LEANDRE 2-derived water vapor mixing ratio measurements are made with a precision better than 0.5 g kg^{-1} in the lower troposphere (i.e. between the surface and the altitude of the aircraft). The data shown in this paper was processed to yield a 300 m vertical resolution and a 1.4 km along-track resolution (100 averaged profiles for a mean aircraft speed of 140 m s^{-1}).

2.2 Model set-up

Simulated atmospheric fields are generated using MM5 version 3.7 (Grell et al., 1994), coupled with the Noah land surface modeling (LSM) system. Two interactively nested model domains are used, the horizontal mesh sizes being 12 km and 4 km, respectively. Domains 1 (coarser domain) and 2 (finer domain) are represented in Fig. 1. The second domain (centered on Homestead, OK) has been chosen so that it covers the entire flight pattern of LEANDRE 2 (Fig. 2b).

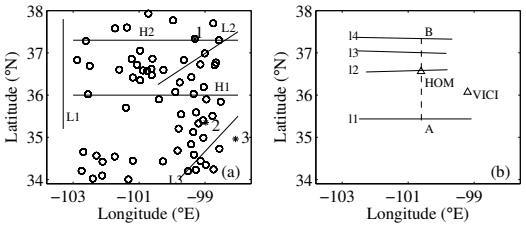

Figure 2: (a) Locations of the surface stations throughout the model domain 2, represented by circles. The solid lines L1, L2, L3 represent the sections studied in details in Section 5. (b) Triangles show the locations of VICI and Homestead (HOM). The solid lines I1, I2, I3 and I4 indicate the flight track of NRL P3 that carried out LEANDRE 2.

The vertical grid is made of 39 half-sigma levels. Since a major objective of the current study is to examine the impact of the surface on the ABL structure and water vapor content, vertical resolution is significantly enhanced in the lower troposphere with 15 levels below 1200 m. A complete set of physics parameterization is used. The ABL scheme used in this simulation is based on that implemented in the NCEP Medium-Range Forecast (MRF) model (Hong and Pan, 1996). The Grell (1993) cumulus parameterization is used on the coarser domain. In model domain 2, this parameterization is not needed since coarse features of convection are explicitly resolved at such high resolution. The radiation scheme is described in Dudhia (1989). An explicit microphysical scheme that predicts rain, snow, graupel, cloud water and cloud ice is used.

The initial and coupling fields were generated by first interpolating the NCEP EDAS analyses available every 3 hours with a 40-km grid resolution onto the 12-km horizontal resolution model grid. The HRLDAS, described by Chen et al. (2004), was run prior to the simulation to obtain fine scale (i.e 4-km horizontal resolution) initial conditions for soil moisture/temperature. HRLDAS makes use of multiple types of observed and analyzed conditions including, 1) NWS Office of Hydrology Stage-IV rainfall analyses performed on a 4-km national grid (Fulton et al., 1998), 2) 0.5º hourly downward solar radiation derived from Geostationary Operational Environmental Satellites (GOES-8 and GOES-9); a product jointly developed by the National Oceanic and Atmospheric Administration (NOAA) National Environmental Satellite Data and Information Service and the University of Maryland (Pinker et al., 2002), 3) near-surface temperature, humidity, wind, downward longwave radiation, and surface pressure from 3-hourly NCEP EDAS analyses, 4) 1-km horizontal resolution United States Geological Survey (USGS) 24-category land use and 1-km horizontal resolution State Soil Geographic (STATSGO) soil texture maps, and 5) 0.15º monthly satellite-derived green vegetation fraction.

The simulation begins at 1200 UT on 29 May 2002 and ends 24 hours later. The model integration for this simulation is short due to a weak synoptic forcing for this day.

3. METEOROLOGICAL AND SURFACE FORCINGS

On 29 May 2002, no significant surface pressure gradient prevails in the investigated area. The environmental situation results in the absence of well established winds near the surface and the meteorological forcing is weak throughout the domain 2. On the contrary, the surface forcing presents some differences throughout the domain 2. On May 28, there is a northeast/southwest oriented accumulated precipitation pattern on the eastern side of the investigated target area due to sparse convective

rainfalls associated with the passage of a front. On May 29, no precipitation occurred throughout the domain 2 (not shown) but the precipitation that occurred the day before generates a east to west soil moisture gradient. In addition, Figure 4 shows the surface fields of vegetation coverage, terrain height and soil types of the investigated area. There is a significant change in vegetation fraction across the domain with a marked east-west gradient, following the terrain elevation gradient. The western half of the domain is mainly grassland (not shown) with a vegetation fraction of about 35-40%. To the east, the vegetation fraction reaches 60%, and savanna becomes the dominant vegetation in the most eastern part of the domain. As opposed to the vegetation fraction, there is no significant soil type gradient from west to east. The soil texture shows much finer-scale structure than the vegetation fraction throughout the domain. In the northern and eastern parts of the domain, including Oklahoma (but not the Oklahoma panhandle), south Kansas and Colorado, the soil composition is dominated by sandy and silt loam (light gray) while in the southern and western parts including the Oklahoma and Texas panhandles, the soil texture is mostly clay loam but with fine scale alternations of parcels with dominant sand texture. The main difference between the soil types is their capability to drain the water and to provide the available water in the soil to the atmosphere. The sand is better drained and then this surface dries faster than clay surfaces.

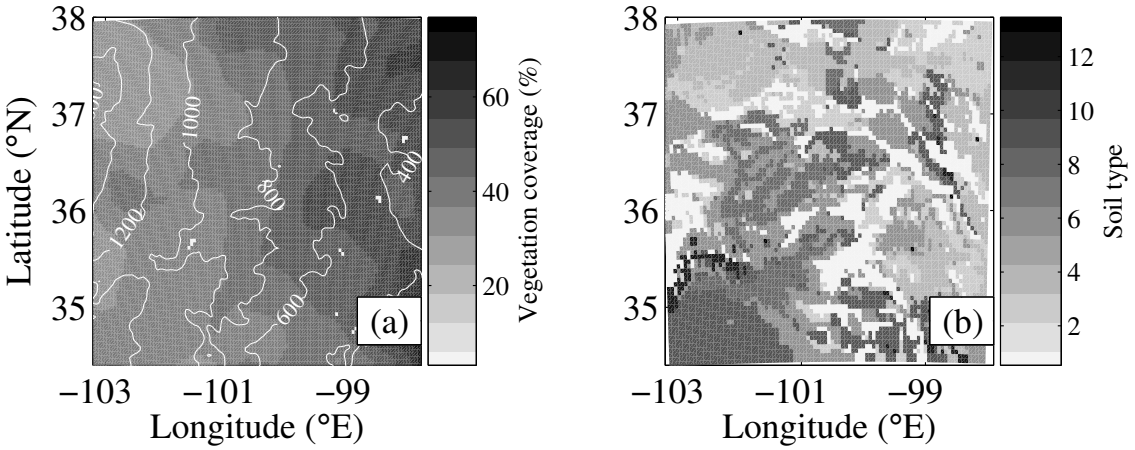

Figure 3: (a) Surface field of the vegetation coverage of domain 2 superimposed with the white contours of terrain height in m. (b) Surface field of the soil type. Light gray colors correspond with Sand, while middle gray indicates Clay Loam and dark gray corresponds with water.

4. DISCUSSION

Figure 4 displays a comparison between the LEANDRE 2 derived water vapor mixing ratio measurements and their simulated counterparts along track l2. The observations clearly show the existence of a well marked west-east gradient for the ABL humidity content. They also indicate the existence of a strong variation of the ABL depth along this leg. The water vapor concentration is accurately simulated (at most 1.5 g kg^{-1} difference in the eastern part of the section), the location of the transition between moist air (> 9-10 g kg^{-1}) and dryer air (< 7-8 g kg^{-1}) is well predicted (at about -101ºE), but the decrease of the ABL depth from 1000 m AGL at -100 ºE down to about 200 m AGL at -101ºE is not reproduced in the simulation. The simulated sensible and latent fluxes along this cross section (not shown) exhibit a variability that is consistent with the observed ABL depth (the sensible heat flux decreases between -100 and -101ºE and increases between -101 and -102ºE). Nevertheless, the benefit of the use of HRLDAS seems to be strongly reduced by the ABL parameterization which tends to smooth the variability of the surface forcing. Note that another boundary layer parameterization, the Mellor-Yamada scheme used in the Eta model (Janjic, 1990; Janjic, 1994), has been tested that do not improve the simulation.

An innovative method to better analyze the role of the surface in comparison with the role of the atmospheric advection in the observed variability of the atmospheric water vapor and the ABL structure is to consider the correlations between variables that characterize the state of the surface (for instance, soil moisture, surface fluxes, vegetation…) and atmospheric variables (for instance 2-m mixing ratio, ABL height). The outputs of the validated simulation are used to compute these correlations.

Figure 5 a, b and c display the interpolated values of 2-m water vapor mixing ratio and the latent heat flux along the three different sections L1, L2, L3 shown in Fig. 2a at 2100 UTC on May

29. These sections have been chosen because they are representative of three different areas of the domain. The values of the data are rescaled for a clearer visualization and arbitrary units are used. Figure 5 shows that the correlations between the 2-m humidity and the latent heat flux strongly depend on the investigated area within domain 2. Along L1, in the western part of the domain, no correlations appear between the 2-m humidity and the latent heat flux, where the atmospheric humidity is weak. Indeed, the 2-m humidity decreases between 36 and 36.5ºN while the latent heat flux is nearly constant on average. The absence of humidity available from the soil and the dry the atmosphere lead to this situation.

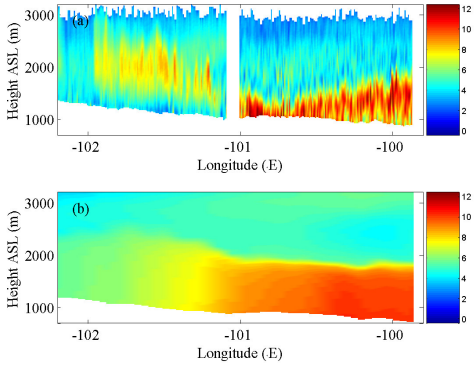

Figure 4: Vertical cross section of water vapor mixing ratio derived from LEANDRE 2 (a) and simulated by MM5 (b) along the line l2 shown on Fig. 2b at about 1800 UTC.

In the southeastern part of the domain (Fig 5c), no correlations exist along the line L3 while the 2-m humidity is higher than in the western part of the domain, The latent heat flux and the 2-m water vapor mixing ratio both decrease between longitude -100 and -99.5ºE, but just after, the surface flux increases significantly while the mixing ratio goes on decreasing. The conclusion is that the surface forcing is not predominant on this part of the domain, and the ABL water vapor content is probably not driven by the surface but by the atmospheric advection.

Along line L2 (panel b), the correlation coefficient is significant (0.78). Two different scales are discernable with large-scale variations inducing large amplitude of variations (between 0 and 1) and smaller-scale variations inducing smaller amplitude of variations. These two scales can be separated using a polynomial function that fits the mean model line. The order of the polynomial function is chosen so that the resulting function fits well with the large scale variations of the model curve. The polynomial function is then reproduced to show the large scale variations while the smaller scale variations are represented by deducting the polynomial function from the model line. Figure 6 displays the correlation between the 2-m humidity and the latent heat flux (upper row), the vegetation (middle row) and the soil moisture (lower row), at small scales (left column), i.e 20-30 km and larger scale (right column), i.e 100-150 km. Table 1 indicates the correlation coefficients between these variables at the two different scales. Fig. 6 and Table 1 show that the surface water vapor mixing ratio and the latent heat flux are strongly correlated at both scales along the line L2. When latent heat flux increases, more humidity is injected from the surface to the ABL. The large scale variations of the latent heat flux and the 2-m humidity are mainly driven by the scale of variations of the vegetation, but we can see that the soil moisture also has an impact on the latent heat flux and the 2-m humidity at this scale (about 100 km). Indeed, westwards from -100ºE, while the vegetation coverage is inferior to 40%, the soil moisture is high (about 0.4 m^3 m^{-3}) and likely explains the large value of 2-m humidity (13-14 g kg^{-1}). On the contrary, no small variations of the vegetation appear and the vegetation can not explain the small scale variability. These small scale variations correspond with the scale of the soil type heterogeneities, with alternations of sand and loam that induce the small scale variations of soil moisture a few hours after the precipitations.

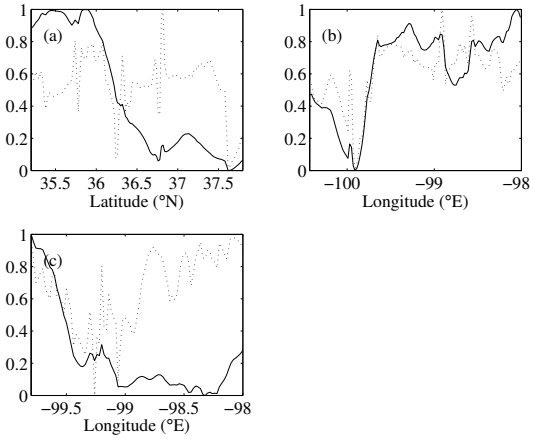

Figure 5: Interpolated values of 2-m water vapor mixing ratio in solid line and the latent heat flux in dotted line on May, 29th, at 2100 UTC along the sections L1 (a), L2 (b) and L3 (c) shown on Fig 2a. The values of the data are rescaled for a clearer visualization and arbitrary units are used.

These different behaviors of the atmosphere in response to the surface forcing will allow to better analyze the reasons of the strong ABL heterogeneity observed along the LEANDRE 2 legs.

	Small scale	Large scale
2-m humidity vs	0.75	0.88

latent heat flux		
2-m humidity vs vegetation	-0.04	0.72
2-m humidity vs soil moisture	0.21	0.14

Table 1 : Correlations coefficient between 2-m humidity and latent heat flux, vegetation and soil moisture on May, 29th at 21 UTC along line L2 at small scale and large scales. The coefficient is significant when the value is higher than 0.2 or lower than -0.2.

5. CONCLUSION

This work uses a validated simulation to better understand the observed variability of the atmospheric water vapor and of the ABL structure. It focuses on the role of the surface to explain this variability. This study aims at identifying the sources of the atmospheric water vapor using an innovating way, based on the correlations between the forcing that characterize the condition of the surface and the atmosphere. It shows that a necessary condition for the surface to play a role in the ABL is to be a source of water vapor (by the way of soil moisture or vegetation). But it is not a sufficient condition, because the atmospheric advection plays an important role also. When correlations exist, the vegetation coverage seems to have a more important impact than the soil moisture. Also the scales of variation of these two variables are different since the soil moisture is strongly modulated by the soil types whose scale of variations is about 20-30 km, while the typical scale for the vegetation fraction variation is about 100 km. So, the large scale variations of the vegetation coverage induce high amplitude variations of ABL height or 2-m water vapor mixing ratio, while the smaller scale variations of soil types induce weaker variations in the atmosphere.

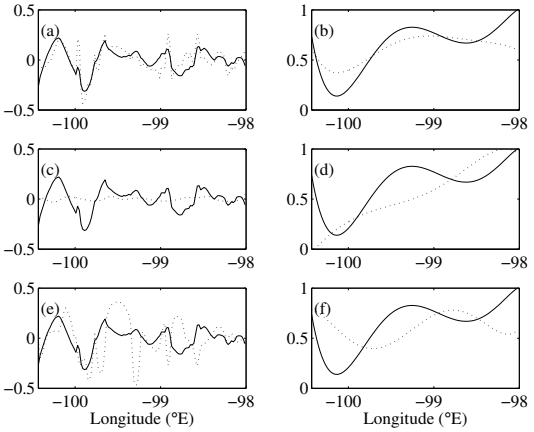

Figure 6: Interpolated values of 2-m water vapor mixing ratio in solid line and the latent heat flux (upper row), the vegetation coverage (middle row) and the soil moisture (lower row) in dotted line on May, 29th, at 2100 UTC along the sections L2 shown in Fig 2a. The small scale variations are represented in the left column, while larger scale variations are in right column .The values of the data are rescaled for a clearer visualization and arbitrary units are used.

ACKNOWLEDGEMENT

This work was partly conducted at Service d'Aéronomie and Laboratoire de Météorologie Dynamique of the Institut Pierre Simon Laplace. A portion of this research was also supported through an NCAR USWRP grant.

Gratitude is bestowed upon Damien Josset for his help to this study.

REFERENCES

Bruneau, D., P. Quaglia, C. Flamant, M. Meissonier and J. Pelon, 2001 : Airborne lidar LEANDRE II for water-vapor profiling in the troposphere. *Appl. Opt.*, **40**, 3450-3475.

Chen, F., K. W. Manning, D. N. Yates, M. A. LeMone, S. B. Trier, R. Cuenca, and D. Niyogi, 2004: Development of a High Resolution Land data Assimilation System (HRLDAS). Preprints, *16th Conference on Numerical Weather Prediction,* Seattle, WA, Amer. Meteor. Soc., CD-ROM, 22.3.

Dudhia, J., 1989: Numerical study of convection observed during the winter monsoon experiment using a mesoscale two-dimensional model. *J. Atmos. Phys.,* **46**, 3077-3107.

Grell, G. A., 1993: Prognostic evaluation of assumptions used by cumulus parameterizations. *Mon. Wea. Rev.*, **121**, 764-787.

Grell, G. A., J. Dudhia and D. R. Stauffer, 1994: A description of the fifth generation Penn State/NCAR mesoscale model (MM5). NCAR technique Note, NCAR/TN 398+STR, 138 pp.

Hong, S.-Y., and H.-L. Pan, 1996: Non local boundary layer vertical diffusion in a medium-range forecast model. *Mon. Wea. Rev.*, **124**, 2322-2339.

Janjic, Z. I., 1990: The step-mountain coordinate: physical package. *Mon. Wea. Rev.*, **118**, 1429-1443.

Janjic, Z. I., 1994: The step-mountain eta coordinate model: further development of the convection, viscous sublayer, and turbulent closure schemes. *Mon. Wea. Rev.*, **122**, 927-945.

Poberaj, G., A. Fix, A. Assion, M. Wirth, C. Kiemle and G. Ehret, 2002: Airborne all-solid-state DIAL for water vapour measurements in the tropopause region: System description and assessment of accuracy. *Appl. Phys.*, **B75**, 165-172.

Weckwerth, T. M., J. W. Wilson and R. M. Wakimoto, 1996: Thermodynamic variability within the convective boundary layer due to horizontal convective rolls. *Mon. Wea. Rev.*, **124**, 769-784.

Weckwerth, T. M. et al., 2004: An overview of the International H_2O Project (IHOP_2002) and some preliminary highlights. *Bull. Amer. Meteor. Soc.,* **85**, 253-277.